CityZen

megaCITY - Zoom for the Environment

Collaborative Project

7th Framework Programme for Research and Technological Development

Cooperation, Theme 6:

Environment (including Climate Change)

Grant Agreement No.: 212095

Deliverable D2.3.1, type R

Report on climate induced changes in air quality and chemical composition on different scales

Due date of deliverable: project month 34

Actual submission date: project month 36

Start date of project: 1 September 2008 Duration: 36 months

Name of lead beneficiary for this deliverable: UiO

Scientist(s) responsible for this deliverable: Frode Stordal, Øivind Hodnebrog

Contributing authors: Frode Stordal (UiO), Øivind Hodnebrog (UiO), Michael Gauss (met.no), Agnes Nyiri (met.no), Svetlana Tsyro (met.no), Peter Wind (met.no), Jan Erik Haugen (met.no), Cornelia Richter (FZJ), Angelika Heil (FZJ), Martin Schultz (FZJ)

Project co-funded by the European Commission within the Seventh Framework Programme (2007-2013)		
Dissemination Level		
PU	Public	X
PP	Restricted to other programme participants (including the Commission Services)	
RE	Restricted to a group specified by the consortium (including the Commission Services)	
CO	Confidential, only for members of the consortium (including the Commission Services)	

Climate induced changes in air quality and chemical composition on different scales

We have estimated the impact of climate change on the chemical composition of the troposphere due to changes in climate from current climate (2000-2010) looking 40 years ahead (2040-2050).

Two offline-coupled studies have been performed, i.e. two chemical transport models were driven by climate data provided by climate models. The climate projections were made by the ECHAM5 and HIRHAM models and followed by chemistry-transport modelling using a global model, Oslo CTM2, and a regional model, EMEP. In this report we focus on carbon monoxide (CO), surface ozone (O_3), and particulate matter, which are measures of primary and secondary air pollution.

In parallel we have estimated the change in the same air pollutants resulting from changes in emissions over the same time period. Both studies used the GEA emission data provided by IIASA for present and future time slices.

Section 1 will describe the ECHAM5/OsloCTM2 study, while section 2 presents results from the HIRHAM/EMEP study. Section 3 provides conclusions.

1) The effect of climate change on air quality, calculated with the ECHAM5/OsloCTM2 model system

Changes in climate from 2000-2010 to 2040-2050 predicted by the ECHAM5 model

ECHAM5 has been run for this study in CityZen from year 2000 to year 2050. It was run using pre-calculated sea surface temperatures (SST) from a coupled climate model run with ECHAM5/MPIOM from the IPCC AR4 assuming emissions of greenhouse gases and aerosols according to scenario A1B. The A1 storyline and scenario family describes a future world of very rapid economic growth, global population that peaks in mid-century and declines thereafter, and the rapid introduction of new and more efficient technologies. Major underlying themes are convergence among regions, capacity building and increased cultural and social interactions, with a substantial reduction in regional differences in per capita income. The A1 scenario family develops into three groups that describe alternative directions of technological change in the energy system, where A1B assumes a balance across all energy sources. Temperatures increase in the 40 year period from 2000-2010 to 2040-2050 in the troposphere and decrease in the stratosphere, in agreement with known impacts of greenhouse gases (Figure 1). The warming, in Northern Hemisphere summer, was in general larger over continents than oceans, and with marked warming at high latitudes. There are also regions with cooling, most noticeably over the North Atlantic Ocean. In parts of Europe and China regional cooling from aerosols is evident, opposing the large scale warming due to the greenhouse gases. However, at mid latitudes there is in general a weaker warming than at both lower and higher latitudes, extending through most of the troposphere and even in both hemispheres.

As expected, a warmer troposphere in 2040-2050 has a higher specific moisture (Figure 2). This is most clearly seen in the tropics. The pattern of moistening to a large extent follows the pattern of warming, so that e.g. Europe will gain less moisture than northern Asia, and in China some regions will even be drier than during current conditions. Temperature changes impact chemistry directly as

most chemical reactions are temperature dependent. Atmospheric moisture is important as OH is formed from water vapour.

Other parameters in the water cycle that impact the atmospheric chemistry are precipitation and cloud cover, regulating wet deposition of water soluble chemical species and thus radiative transfer and photo-dissociation rates respectively. Changes in these two parameters are clearly related to atmospheric moisture and also to each other, as seen in Figures 3 and 4. In the tropics the Hadley cell is somewhat displaced, yielding changes in tropical and subtropical precipitation and cloud cover. At low and mid latitudes, the fraction of mid and high level clouds decreases, whereas there is an increase in the fraction of low level clouds. The low level clouds increase their fraction in parts of Europe, whereas they decrease their fraction in other parts. Over India there is a noticeable decrease in precipitation as well as in cloud fraction. In China precipitation increases in the central and southern parts, whereas there is a drying in the north. Low level clouds follow the same pattern, with increased cloudiness in the south and decreased in the north.

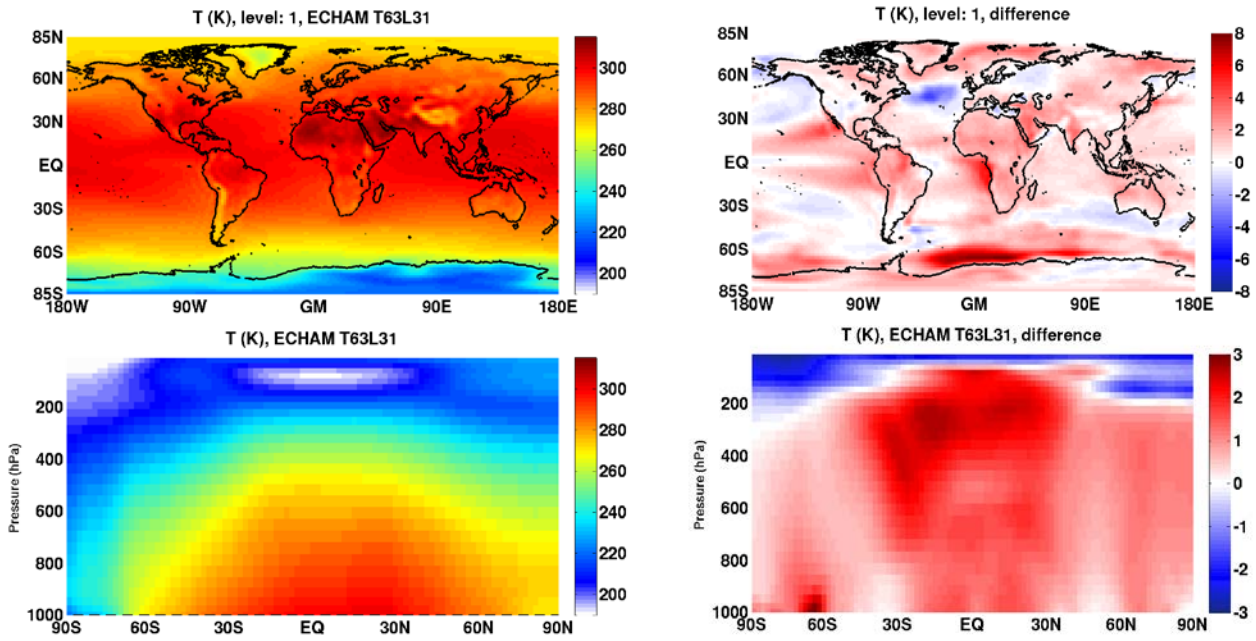

Figure 1: Temperature (K) as 11-year averages for the northern hemisphere summer (June, July, August) shown for the period 2000-2010 (left) and as differences between the periods 2040-2050 and 2000-2010 (right) for near-surface (top) and zonal mean (bottom). Note that the scales are different.

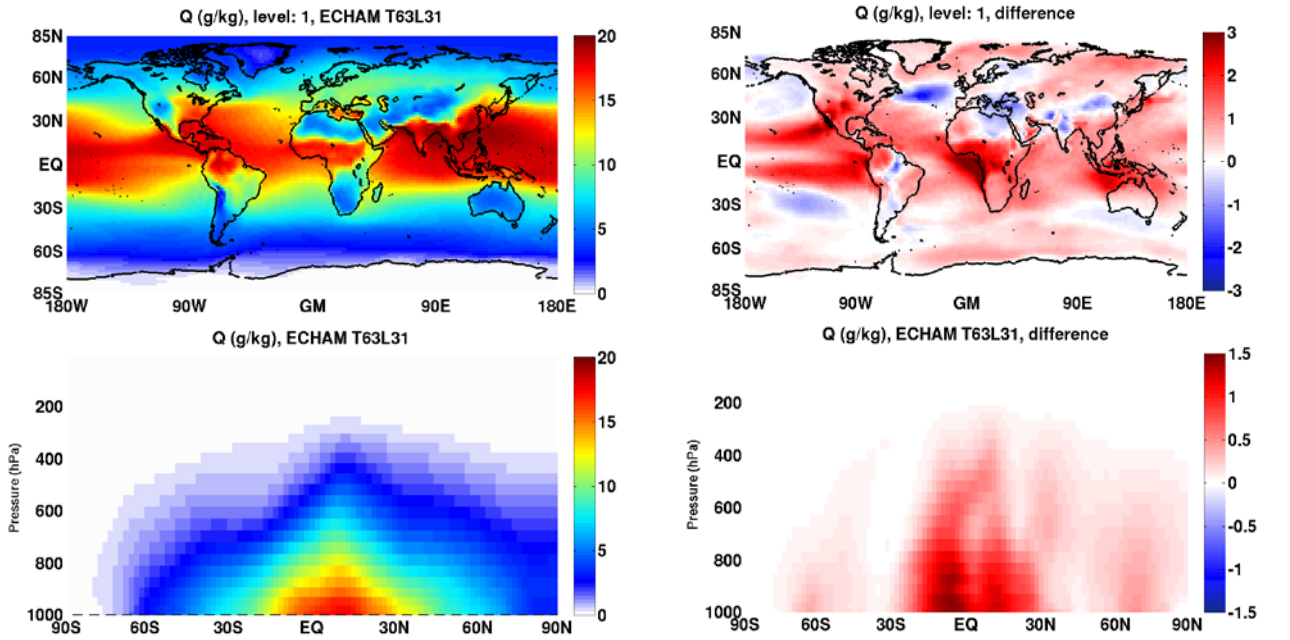

Figure 2: Specific humidity (g/kg) as 11-year averages for the northern hemisphere summer (June, July, August) shown for the period 2000-2010 (left) and as differences between the periods 2040-2050 and 2000-2010 (right) for near-surface (top) and zonal mean (bottom). Note that the scales are different.

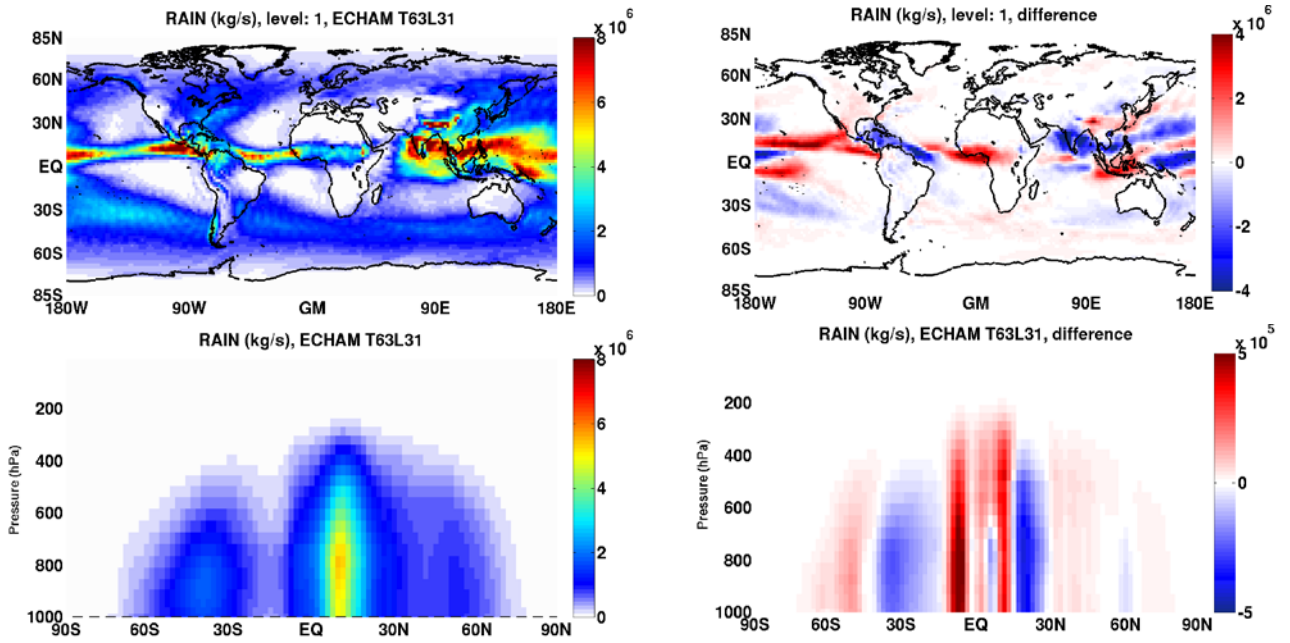

Figure 3: Precipitation flux (kg/s) as 11-year averages for the northern hemisphere summer (June, July, August) shown for the period 2000-2010 (left) and as differences between the periods 2040-2050 and 2000-2010 (right) for near-surface (top) and zonal mean (bottom). Note that the scales are different.

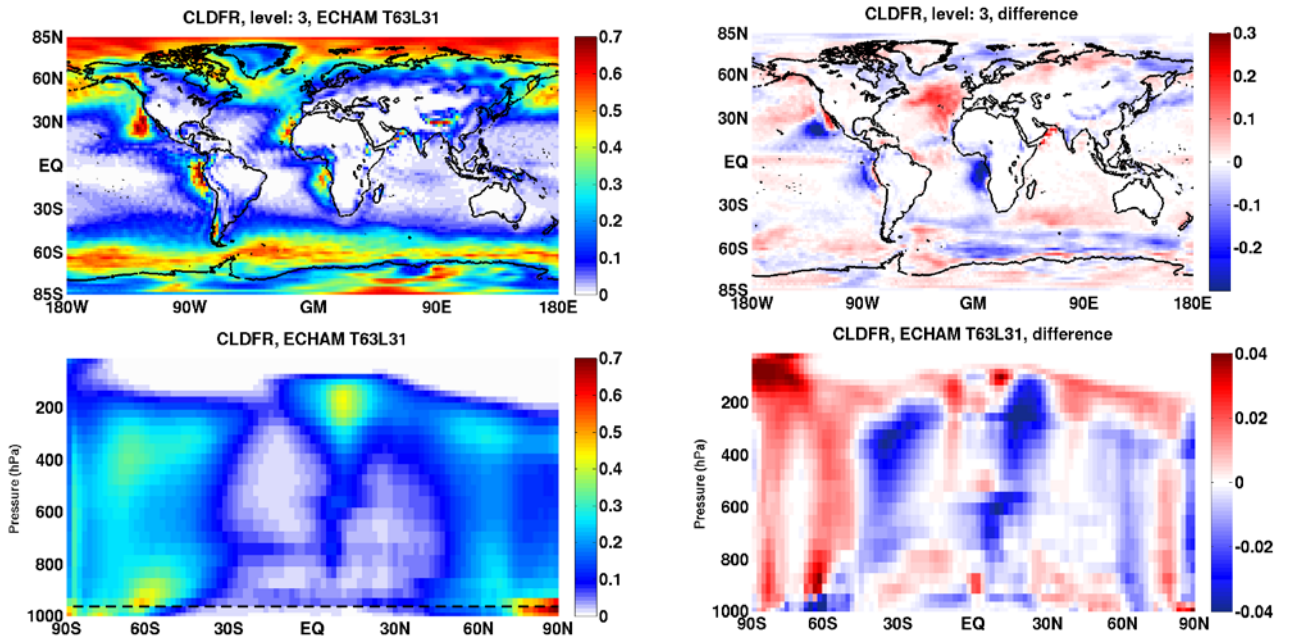

Figure 4: Cloud fraction (0-1) as 11-year averages for the northern hemisphere summer (June, July, August) shown for the period 2000-2010 (left) and as differences between the periods 2040-2050 and 2000-2010 (right) at the 950 hPa level (top) and in the zonal mean (bottom). Note that the scales are different.

Changes in anthropogenic emissions from 2005 to 2050

To put the changes in atmospheric chemistry due to climate change in perspective we have estimated also the changes in chemistry due to changes in anthropogenic emissions. We have selected the HIGH-CLE scenario for this purpose. This scenario assumes full implementation of all current and planned air pollution legislation world-wide until 2030. Thus it provides a measure of the impact of current and planned air pollution policies. However, no specific climate or energy access policy is assumed.

We clearly see that in Europe emission legislation will result in continued reductions in emissions of CO as well as NOx in the 40 year period studied. All across Europe CO (Figure 5) and NOx (Figure 6) emissions are lower in 2040-2050 than in 2000-2010. We see the same negative trend in CO in China, but emissions of NOx are increasing slightly there. In many developing countries there will be increasing emissions of CO as well as NOx. This change is clearly evident for India (Figure 5 and 6).

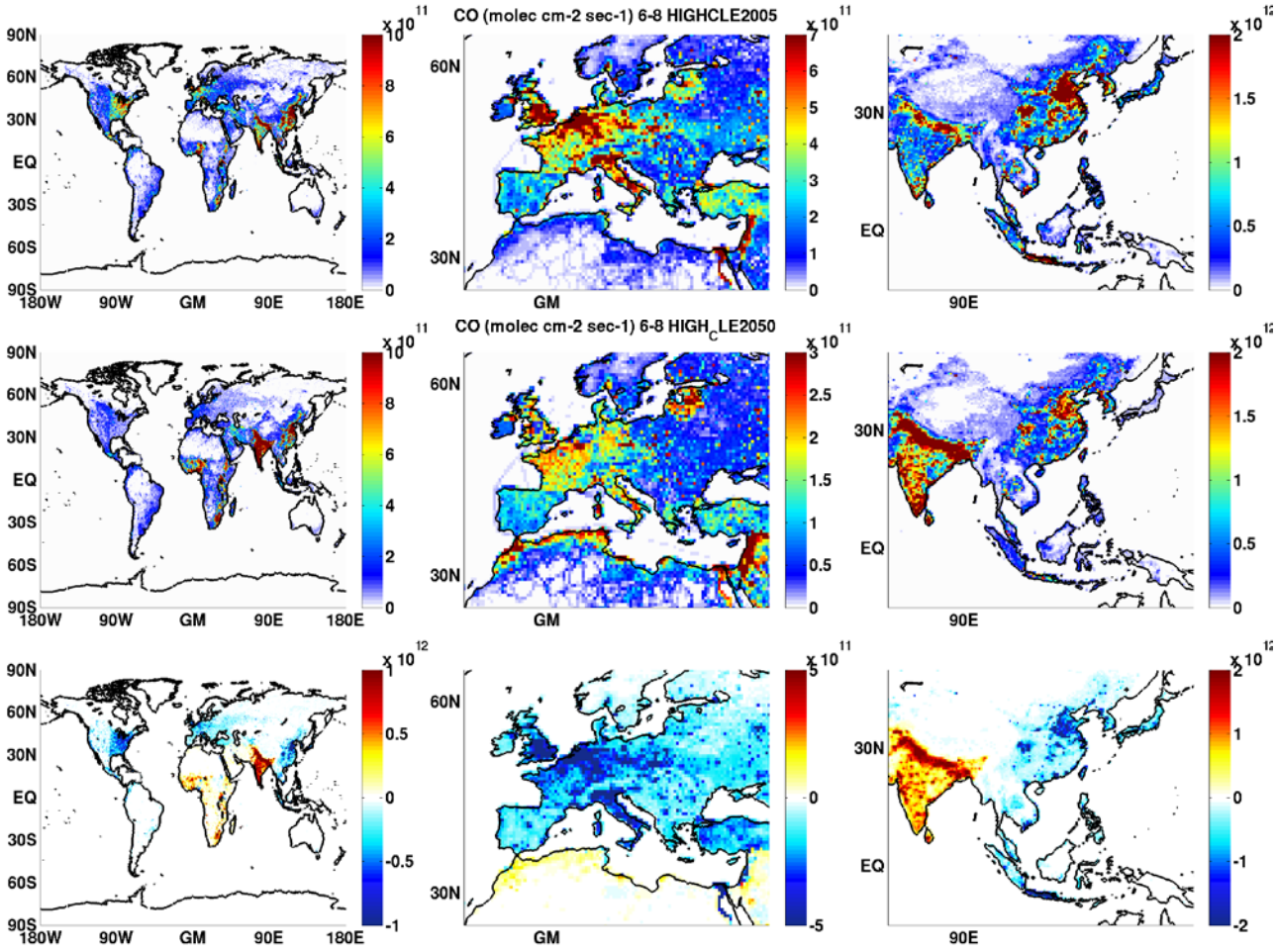

Figure 5: Anthropogenic emissions of CO (molec cm^{-2} s^{-1}) in the period June-August for 2005 (top), for 2050 HIGH CLE (middle), and as differences between the two scenarios (bottom). Note that the scales are different.

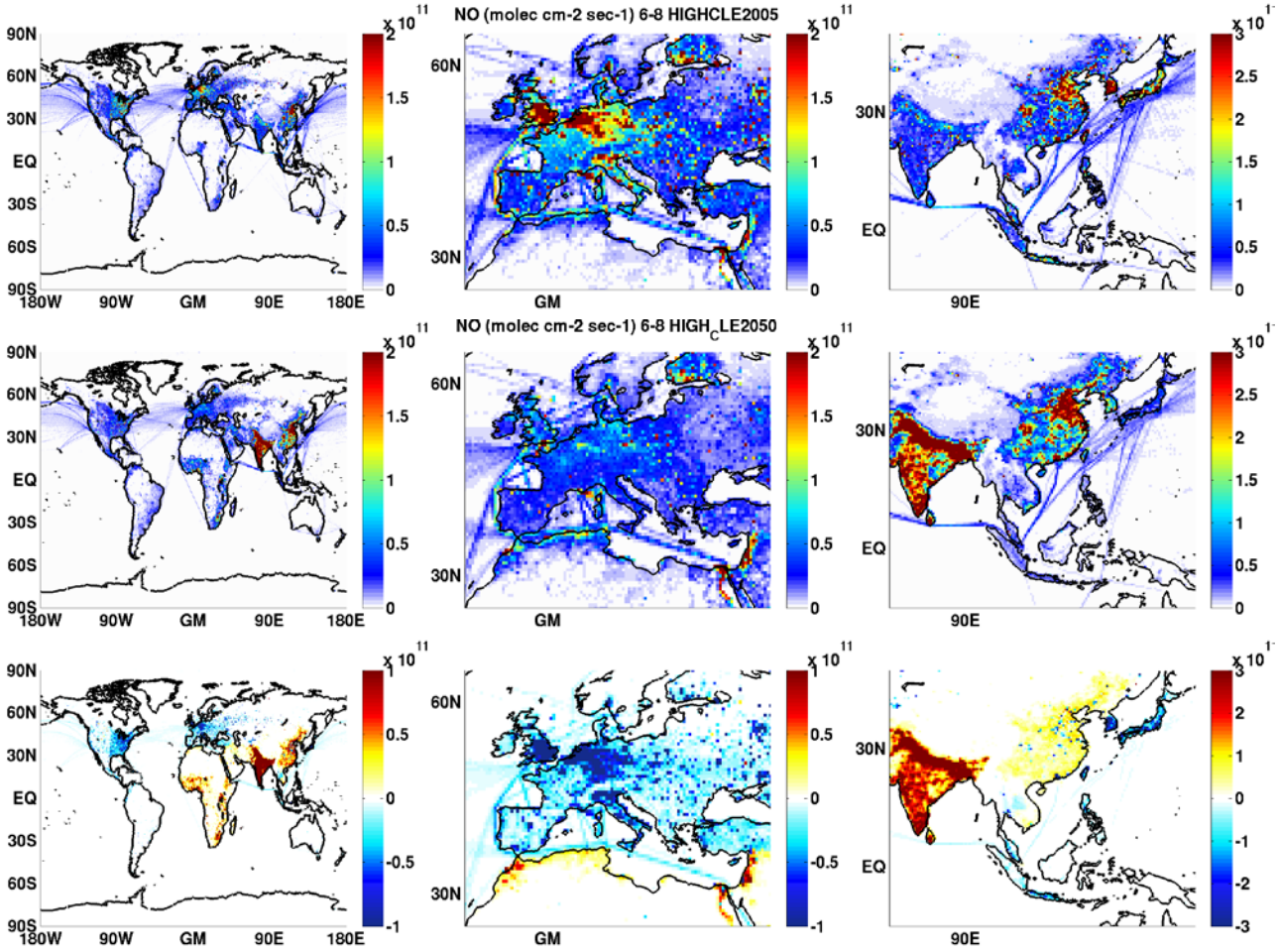

Figure 6: Anthropogenic emissions of NO_X (molec cm^{-2} s^{-1}) in the period June-August for 2005 (top), for 2050 HIGH CLE (middle), and as differences between the two scenarios (bottom). Note that the scales are different.

Changes in CO predicted by the OsloCTM2 model

The Oslo CTM2 model has been run with ECHAM as the meteorological driver. In the past this CTM has only been run with meteorology from the ECMWF. The capability to use ECHAM meteorology has been developed as a part of CityZen. We have run the model both for current (2000-2010) and future (2040-2050) meteorologies. The current conditions were run with both current and future emissions, whereas the future meteorology was run with future emissions, to allow separation of changes in the atmospheric chemistry which are due to the two changes. The estimated changes in CO concentrations are quite similar to the changes in the emissions themselves, at least at the surface which is depicted in Figure 7. However, at higher tropospheric levels the winds are stronger, so that the impacts of anthropogenic emission changes are advected some distance away from the emission changes themselves. The reductions in emissions over Europe lead to similar reduction in CO concentrations there. In a similar way concentrations of CO are reduced over China, but enhanced over India.

Interestingly, the response to climate change is an increase in CO concentration over the wetter parts of Europe and China: This is in contradiction to the fact that the atmospheric moisture content is higher, which would by itself lead to higher concentrations of OH. Likewise, the drying of northern China and northern India leads to decrease in CO concentrations there. Thus, the changes in CO surface concentrations are presumably influenced by also changes in the cloud fraction, with more cloudiness in the wetter regions and less in the drier ones, increasing the production of OH in the drier regions. Figure 7 shows that the signal in CO is stronger from emission changes than from climate changes. This can be seen also in the combined effect, which has a pattern more similar to changes in emissions than climate change. Nevertheless, the impact of climate change is noticeable, and must clearly be taken into account when assessing future CO concentrations in Europe and also other densely populated regions of the world.

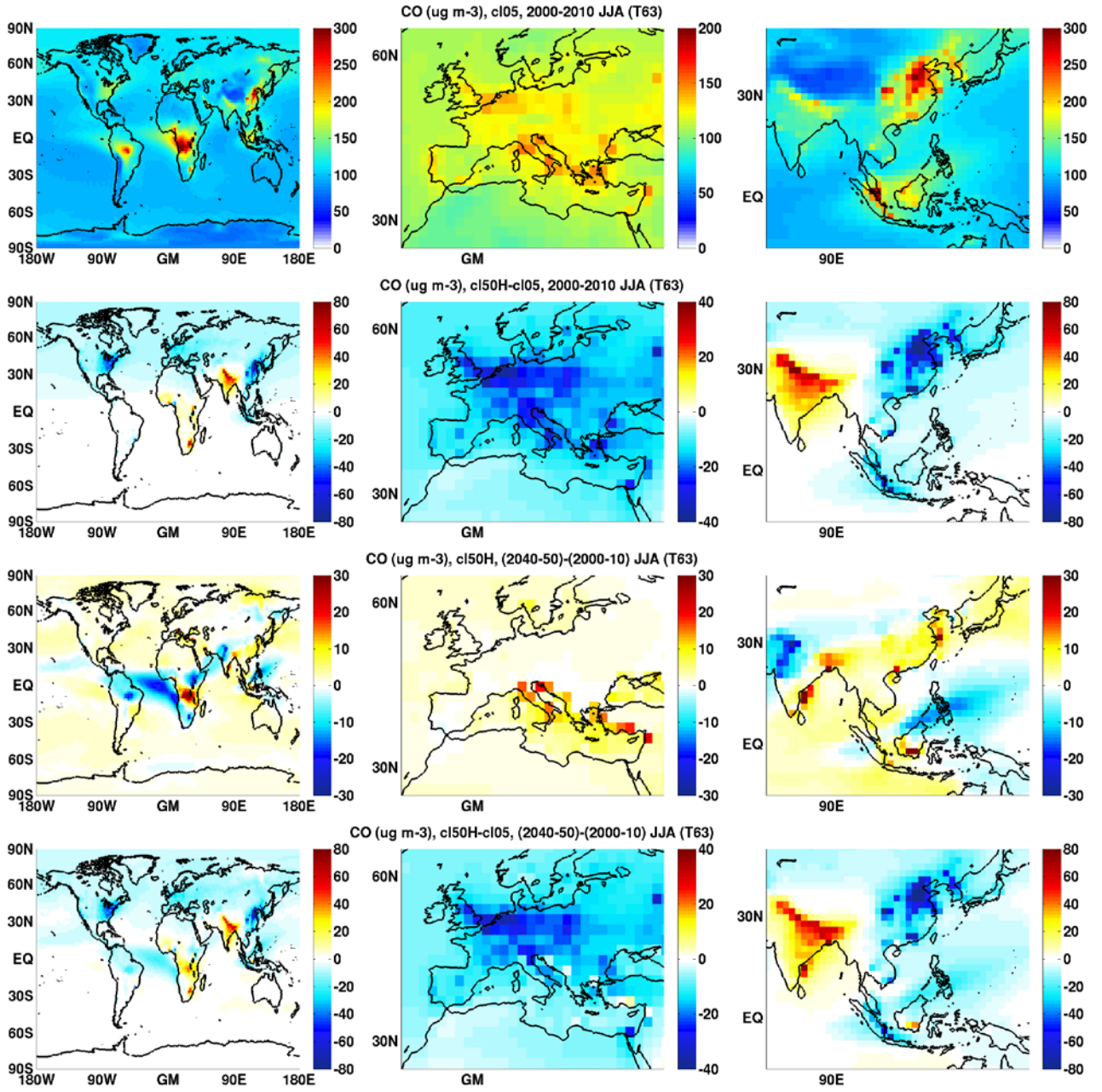

Figure 7: Near-surface CO (µg/m^3) for the northern hemisphere summer (June, July, August), for (i) 2000-2010 conditions (uppermost row); (ii) change due to changes in emissions from 2005 to 2050, the HIGH CLE scenario (second row); (iii) change due to change in climate in the period 2040-2050 (third row); (iv) and the change due to the combined impact of changes in emissions and climate (fourth row).

Changes in ozone predicted by the OsloCTM2 model

The ozone concentrations have been estimated in the same experiments as for CO and the results are shown in Figure 8. As the focus is here on air pollution we concentrate on the daily maximum value of the near surface concentrations. Like the concentrations of CO, ozone responds with reduced concentrations to changes in emissions in 2040-2050. In India, there is in a similar way increase in ozone as emissions increase for both CO and NOx. In China, we assume reductions in CO emissions but enhanced NOx emissions. The result is only weaker changes in ozone, with increase in some and decrease in other regions.

The climate response in ozone is increased surface maximum concentrations over much of the continental parts of the world. The impact of climate change is very complex, involving all the meteorological parameters discussed above, and even more, e.g. the boundary layer depth and mixing. In Europe, the largest increases in ozone are found in the Mediterranean region, with some hot spots which could be attributed to forest fires. The fires are assumed to have similar geographical and temporal distributions in the future (2040-2050) world, and apparently the meteorology is changed when we assume fires in the future. This particular feature is not realistic as the conditions for setting up fires will also change. However, what is not taken into account in our calculations is the fact that fire probability will increase in a future dries Mediterranean region. Thus our estimate represents probably lower limit values. In Figure 9 we depict the year to year variability in surface ozone daily maximum. We see that the increase in ozone in the Mediterranean region is somewhat larger than the interannual variability. Ozone increases also in much of southern and central China as well as the southern and eastern parts of India. Like in the case of CO, the impacts of changes in emissions are somewhat more pronounced than those due to climate change. Consequently in the combined effect we recognize the emission effect most clearly. However, the impact of climate change is clearly noticeable, and must be taken into account when assessing future impacts on e.g. human health and agricultural production

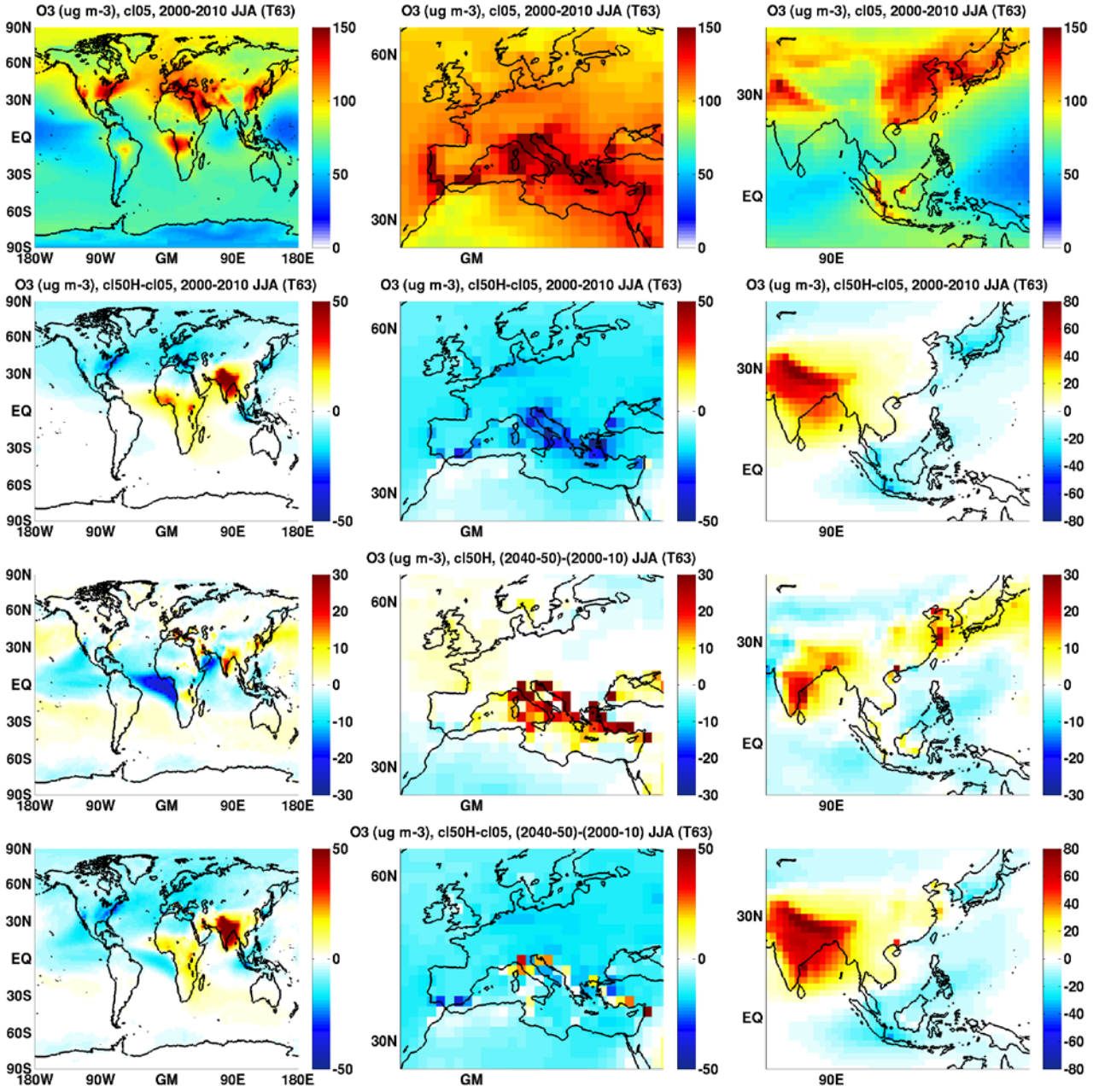

Figure 8: Near-surface ozone (µg/m^3) for the northern hemisphere summer (June, July, August), for (i) 2000-2010 conditions (uppermost row); (ii) change due to changes in emissions from 2005 to 2050, the HIGH CLE scenario (second row); (iii) change due to change in climate in the period 2040-2050 (third row); (iv) and the change due to the combined impact of changes in emissions and climate (fourth row). All estimates are for daily maximum ozone.

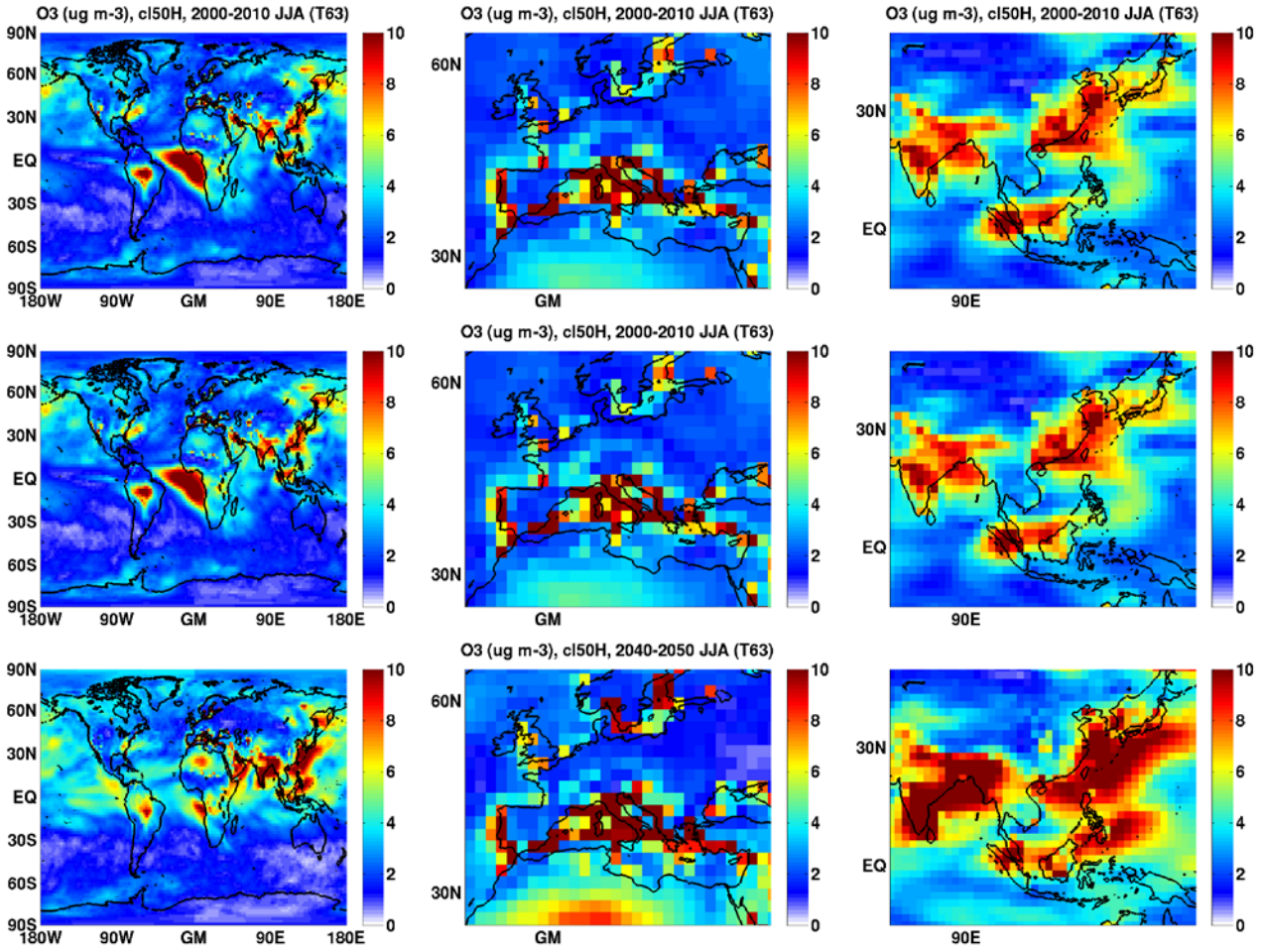

Figure 9: Absolute standard deviation over 11 years in near-surface ozone (µg/m^3) for the northern hemisphere summer (June, July, August), for (i) 2000-2010 conditions (uppermost row); (ii) 2000-2010 conditions with emissions from 2050, the HIGH CLE scenario (second row); and (iii) 2040-2050 conditions with emissions from 2050, the HIGH CLE scenario (third row). All estimates are for daily maximum ozone.

2) The effect of climate change on air quality, calculated with the HIRHAM/EMEP model system

This study was performed at met.no using a regional climate model and a regional chemical transport model. Figure 10 shows the basic experimental setup, which is quite similar to the setup of the UiO/FZJ calculation described in Section 1. The EMEP/Meteorological Synthesizing Centre - West (MSC-W) model (hereafter refered to as 'EMEP model') used present and future emission data provided by IIASA. The meteorological data were generated through dynamical downscaling using model output from the Hadley global climate model HadCM3 and applying the regional climate model HIRHAM. The climate models used greenhouse gas emissions as specified in the SRES A1b scenario of IPCC (Nakicenovic and Swart 2000).

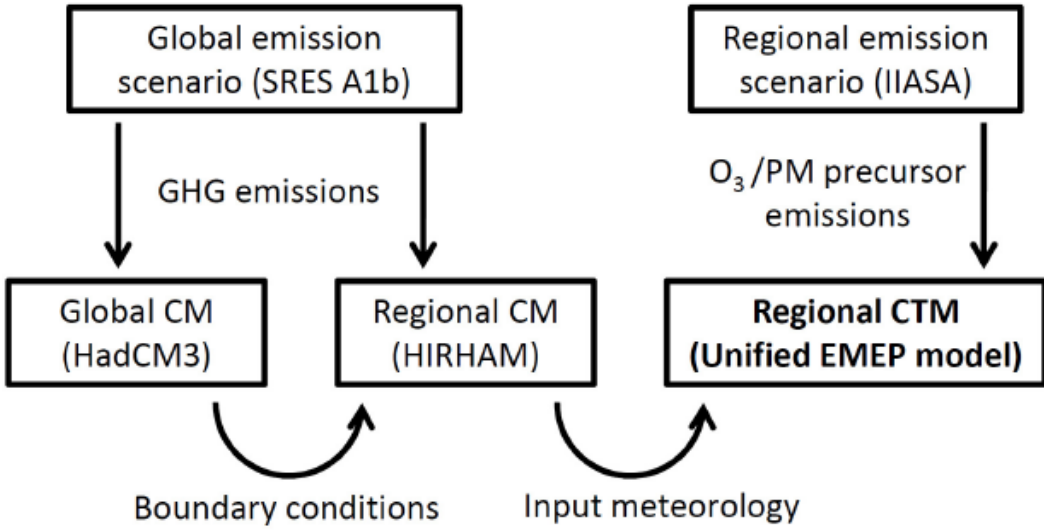

Figure 10: Experimental setup for studying effects of climate change on air quality in a CTM. (CM: Climate Model, CTM: Chemical Transport Model. 'Unified EMEP model' = EMEP model)

Changes in climate from 2000-2010 to 2040-50 predicted by the HIRHAM model

Meteorological input data to the EMEP model for this experiment were generated using a dynamic downscaling approach. The regional climate change scenario was produced within the Nordic Climate and Energy Systems (CES) project and the European FP6 project ENSEMBLES (van der Linden and Mitchell 2009). The joint ENSEMBLES/CES regional climate model (RCM) ensemble consists of more than 25 RCM simulations (see http://ensemblesrt3.dmi.dk/extended_table.php) covering most of Europe at 25 km horizontal resolution. All RCM scenarios are based on the SRES A1B emission scenario (Nakicenovic and Swart 2000).

The particular ensemble member used to generate data for the EMEP model runs was produced by the HIRHAM RCM (Haugen and Haakenstad 2006, Haugen and Iversen 2008). This HIRHAM run was forced by data from the Hadley Centre global climate model HadCM3. The HadCM3 data was run at the Hadley Centre on 3.75º (lat) × 2.5º (lon) resolution with emissions from SRES A1B. The HIRHAM RCM was run on a rotated spherical projection with 0.22º × 0.22º horizontal resolution for the period 1950-2050. All meteorological parameters required by the EMEP model were ex-

tracted from this 101-year HIRHAM data set, interpolated into the vertical grid of the EMEP model and converted into netCDF format.

We have run two 11-year periods, 2000-2010 and 2040-2050, to look at future air quality taking into account climate change. Figure 11 shows differences in temperature and surface precipitation averaged over the two 11-year periods, for the JJA (June/July/August) and the DJF (December/January/February) seasons, as seen in the HIRHAM data. The temperature increase from the 2000s to the 2040s is clearly seen in nearly all parts of Europe, North Africa and the European Arctic. The highest temperature increase occurs during winter in high latitudes, while in mid-latitudes the warming is most pronounced during summer. Precipitation is reduced mainly in coastal regions of the Mediterranean, the Bay of Biscay and some regions in the Alps. Largest increases in precipitation are seen during winter in Western Scandinavia and the Eastern part of the North Atlantic.

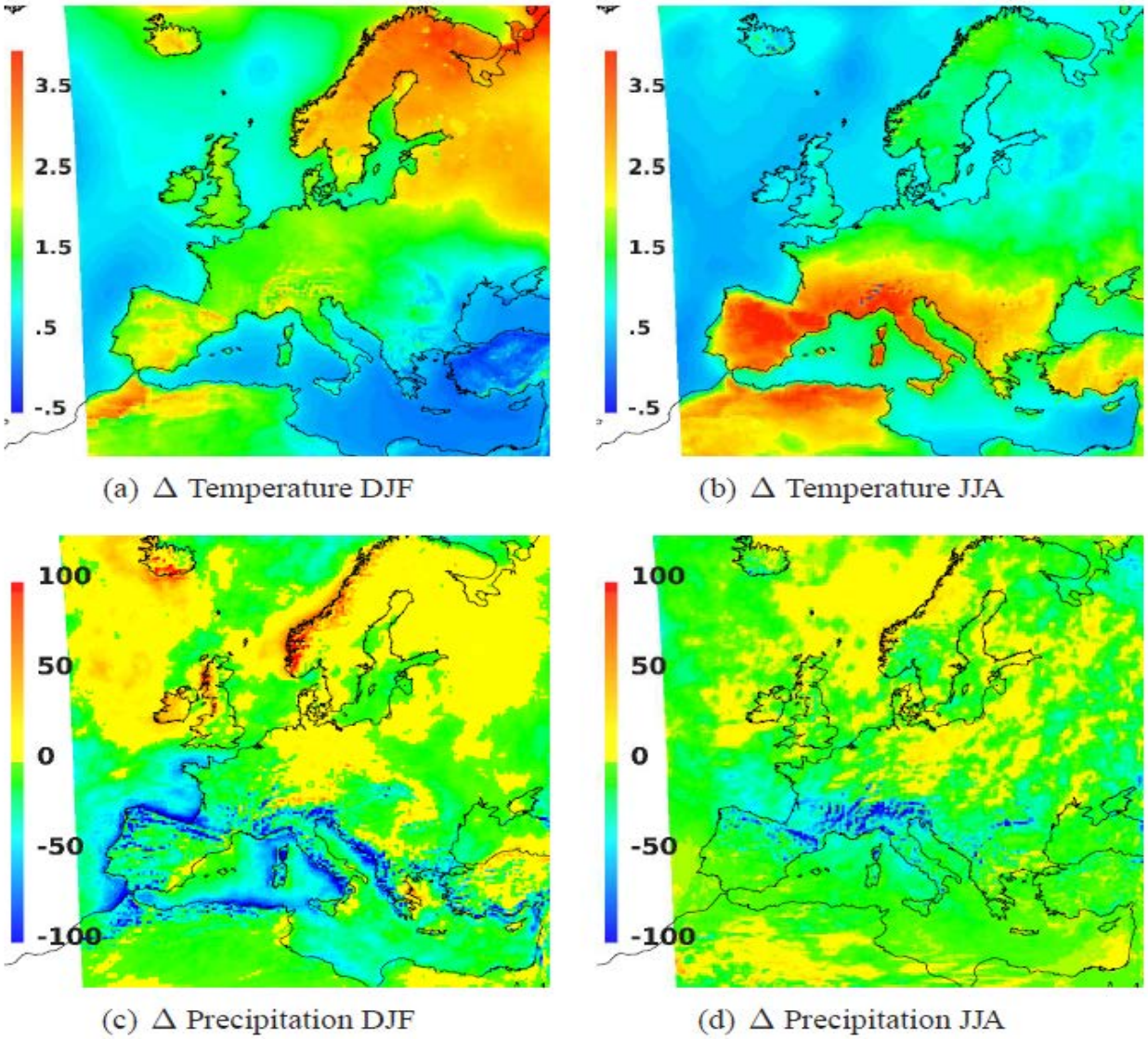

Figure 11: Change in T (a,b) and surface precipitation (c,d) between the 2000s and the 2040s for the JJA and the DJF seasons. Units: Kelvin for temperature and mm/year for surface precipitation. (In the precipitation plots, dark blue and dark red colors comprise a small number of grid cells with more extreme values, about -400 mm/yr and +300 mm/yr, respectively.)

Emissions

In this study, two sets of emission data have been used, which were derived from two global emission scenarios both developed by IIASA. The first one, HIGH-CLE, is the same as was used by UiO in the calculation described in Section 1:

HIGH-CLE. No specific policies on climate change and energy access are implemented in this scenario. However, it assumes full implementation of all current and planned air pollution legislation world-wide until 2030. Thus, this scenario provides a measure of the impact of current and planned air pollution policies in the absence of any specific climate or energy access policy.

In addition, a more optimistic emission scenario was used, LOW-CLE, that also assumes a stringent climate policy:

LOW-CLE. In this scenario a stringent climate policy corresponding to a 2-degree global temperature target is implemented. In addition, it assumes a moderate energy access policy corresponding to microfinance and 20% fuel subsidy, as well as full implementation of all current and planned air quality legislation until 2030, similar to the reference case described above. Thus, this scenario explicitly provides an indication of the co-benefits of combining policies on climate change, energy access and air pollution.

In both emission scenarios reductions of all pollutants are foreseen, except (NH_3). The LOW-CLE scenario features larger emission reductions than the HIGH-CLE scenario.

Changes in air pollution from 2000-2010 to 2040-2050 predicted by the EMEP model

Table 1 lists the four model simulations performed so far. The first one is a reference simulation for the 11-year period from 2000 to 2010, using HIGH-CLE emissions for the same period. The second model run, S1, uses the same emissions but meteorology for the years 2040 to 2050, i.e. the difference ’S1 minus S0’ represents the effect of predicted climate change alone, not taking into account any change in emissions. The two final simulations, S2 and S3, are two realizations of the situation in the 2040s, based on the emission scenarios HIGH-CLE and LOW-CLE, respectively. The differences ’S2 minus S0’ and ’S3 minus S0’ thus show the effect of emission change and predicted climate change combined.

Name	Meteorology	Emissions
S0	2000, …, 2010	HIGH-CLE 2000, …, 2010
S1	2040, …, 2050	HIGH-CLE 2000, …, 2010
S2	2040, …, 2050	HIGH-CLE 2040, …, 2050
S3	2040, …, 2050	LOW-CLE 2040, …, 2050

Table 1: Overview of the different model runs with the EMEP model.

Changes in surface ozone

Solberg et al. (2008) used the EMEP model and measurements from the EMEP network to investigate surface ozone values over Europe during the extreme summer of 2003. They suggested a num-

ber of positive feedbacks between weather conditions and ozone, which contributed to the elevated surface ozone values during that heat wave. Because of climate change, such heat waves may occur more frequently in the future and may gradually overshadow the effect of reduced emissions from anthropogenic sources of VOC and NOx in controlling surface ozone. For instance, increased UV radiation (during high pressure conditions), extended residence times in stagnant polluted boundary layers, high temperatures destabilizing PAN and increasing biogenic emissions of ozone precursors, as well as reduced deposition on dryer soil all lead to higher ozone levels.

In this calculation we have looked at seasonal or annual averages of daily maximum ozone. According to our results, climate change alone ('S1 minus S0') shifts the frequency distribution of maximum daily ozone, averaged over the summer months, towards higher values (not shown). For instance, the number of grid cells with values of 70 ppb or more increases by about 50% from the 2000s to the 2040s. However, when accounting for emission change according to the LOW-CLE and HIGH-CLE scenarios, we obtain quite different results: Indeed, in the LOW-CLE scenario, the number of grid cells in this category is reduced by a factor of ten.

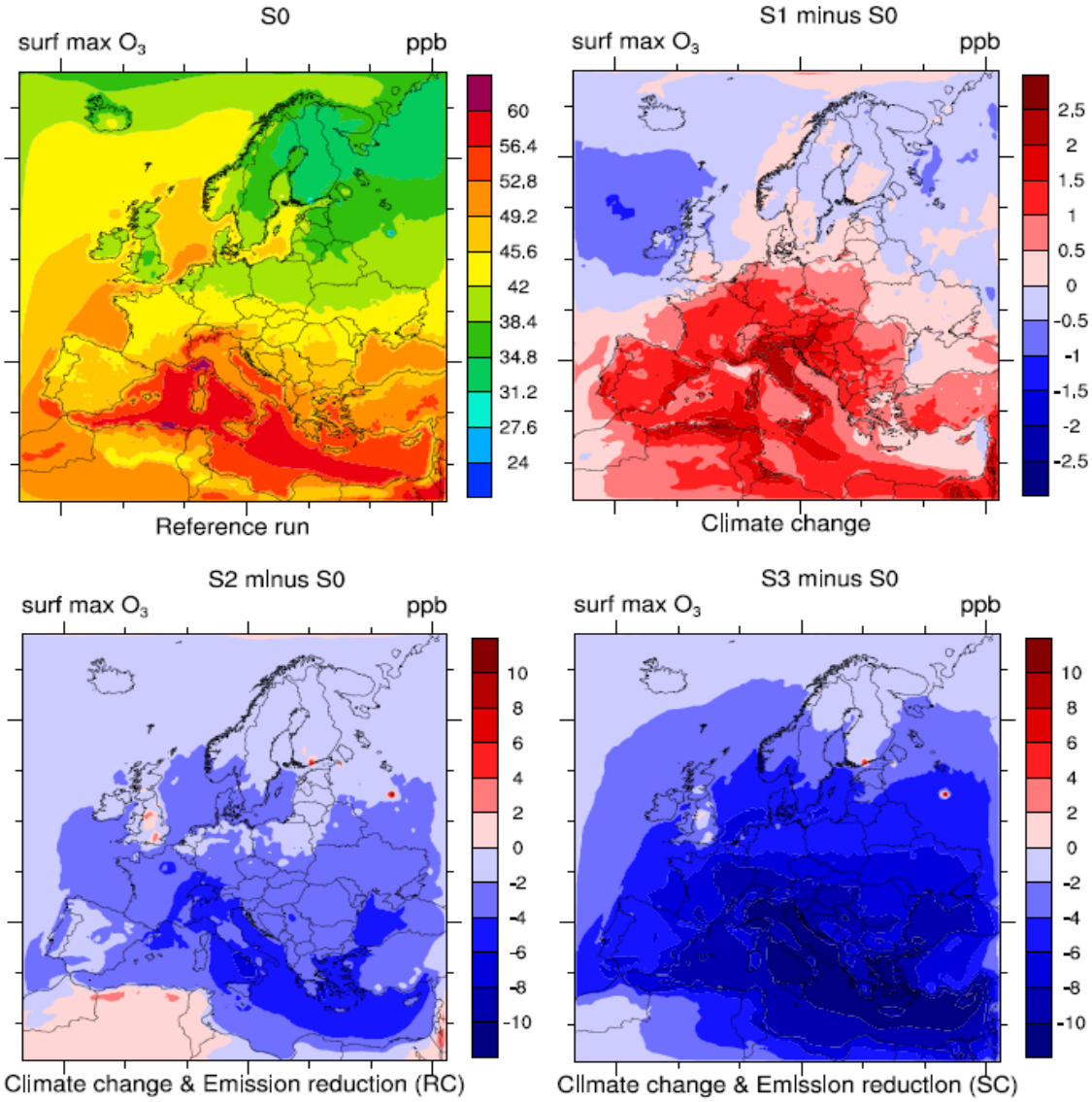

Figure 12: Upper left: Daily maximum near-surface ozone, averaged over the 11-year period 2000 to 2010. The three other plots show changes in daily maximum surface ozone:'S1 minus S0' (upper right), 'S2 minus S0' (lower left), and 'S3 minus S0' (lower right). Unit: ppb.

Figure 12 shows horizontal maps of daily maximum surface ozone in the 2000s and the changes between the 2000s and the 2040s. In this analysis the daily maximum surface ozone values are averaged over the year. The upper left panel shows the well-known maximum values over the Mediterranean and the relatively low values over less polluted and/or less insolated areas in the Northeast of Europe. When taking into account climate change only (upper right panel), daily maximum ozone increases in most areas, especially in the Southern parts of Europe, where temperature increases significantly (and cloudiness decreases) during the summer months with efficient photochemistry. Again, when accounting for projected reductions in emissions in addition, maximum ozone values decrease significantly, as is seen in the two lower panels of the figure, showing the 'S2 minus S0' and 'S3 minus S0' differences, respectively. Not surprisingly, reductions in maximum surface ozone are largest in the most optimistic scenario, S3.

In conclusion, maximum surface ozone is indeed reduced significantly, but the reduction is slightly weakened by the climate change effect. A more thorough analyses would obviously include winds and other meteorological parameters as well. This will be subject for further investigation in the near future.

Changes in aerosols

Both emissions reduction and changes in the meteorological conditions affect aerosol concentrations. In this respect, precipitation is the most important meteorological parameter as most of aerosols are soluble and therefore are subject to efficient wet scavenging. Furthermore, temperature has an effect on the levels of semi-volatile secondary aerosols, like ammonium nitrate and secondary organic aerosols, shifting the equilibrium balance between the gas and aerosol phases. Namely, these aerosols will tend to evaporate/be formed as temperature increases/decreases. Also, a higher relative humidity facilitates the formation of secondary aerosols. The changes in atmospheric stability and wind intensity and patterns will additionally affect aerosol dispersion and dry deposition, but these effects are not considered here. Keeping this in mind, we look closer at the changes in the concentrations of PM2.5, which consists of SIA (the sum of fine SO_4^{2-}, NO_3^- and NH_4^+) and primary PM2.5.

Effects of climate change from the 2000s to the 2040s on PM2.5 include an increase of PM2.5 concentrations in the central and southern parts of Europe and over the Mediterranean Sea, and a decrease in areas further North (Nordic and Baltic countries, north-west of Russia, Belarus, Poland, Ireland) (Figure 13, b). According to our model calculations, the reductions in PM2.5 concentrations are mostly within -0.4 μg m^{-3}, but increases may reach 0.8-1.2 μg m^{-3}. These changes are mostly due to changes in the precipitation regime (Figure 11), which causes less removal by wet scavenging of aerosols in the southern regions, whilst more efficient wet removal in the northern regions. The precipitation influences in a similar way both SIA and PPM2.5 (not shown here), but the effect on SIA is larger than on PPM2.5 due to SIA's higher solubility. The general increase of temperature from 2000s to 2040s is expected to cause some decrease in SIA concentrations (but not PPM2.5). This effect is not pronounced in the southern regions, where the effect of precipitation dominates, but it contributes to the decrease of SIA and PPM2.5 in the northern regions.

The combined effect of climate change and emission reductions in the HIGH-CLE scenario is to reduce PM2.5 by 1 to 4 μg m^{-3} all over and by 4 to 12 μg m^{-3} in Central and South-Eastern Europe and in Northern Italy, as illustrated in Figure 13 (lower left panel). Both SIA and PPM2.5 are reduced in this case. However, the PM2.5 reductions are largely due to reductions in SIA concentrations, as SIA's contribution to PM2.5 is larger compared to PPM2.5.

Even larger emission reductions in line with scenario LOW-CLE bring about further decrease in the concentrations of SIA and PPM2.5, and consequently PM2.5 (Figure 13, lower right panel). With the LOW-CLE emission scenario including climate change, reductions of PM2.5 in the range of 4 to 12 μg m^{-3} are achieved over large parts of Central, Eastern and South-Eastern Europe, i.e. the regions of large emission at present. In less pollutant and remote areas, PM2.5 can be reduced by up to 4 μg m^{-3}, according to the model calculations.

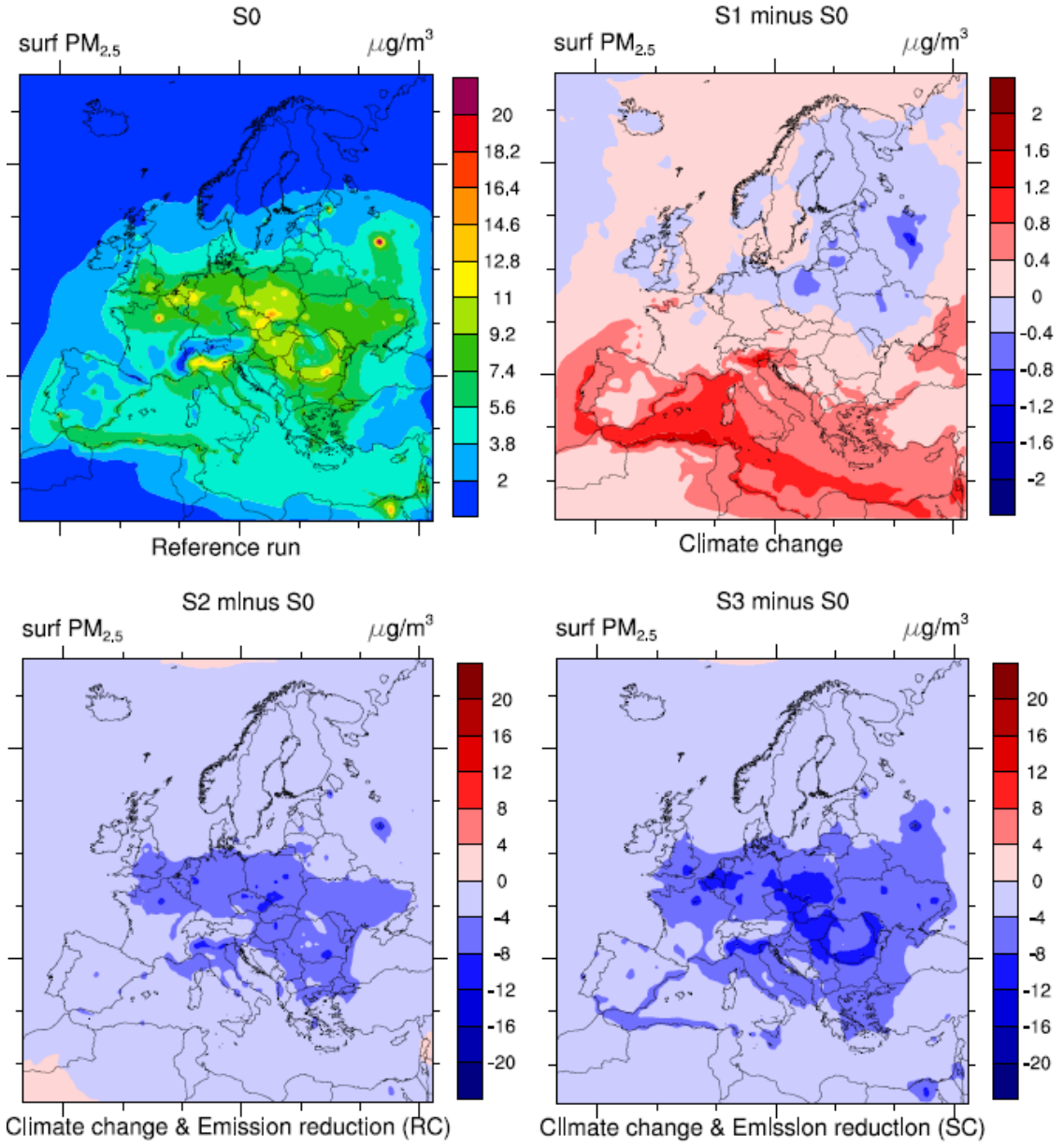

Figure 13: Upper left: Surface concentrations of PM2.5, averaged over the 11-year period 2000 to 2010. The three other plots show changes in surface concentrations of PM2.5: 'S1 minus S0' (upper right), 'S2 minus S0' (lower left), and 'S3 minus S0' (lower right). Unit: μg m^{-3}.

3) Conclusions and future directions

Offline calculations with chemical transport models using climate data from general circulation models have been performed. Changes in air quality due to climate change are clearly visible from

the model runs performed in CityZen. IIASA has provided emission scenarios for the time period 2000-2050. From our calculations it seems that the effects from emission changes are larger than those due to climate change. For example in Europe, climate change alone will lead to an increase in ozone and particulate matter, mainly related to changes in temperature and precipitation. However, these changes are overwhelmed by emission reductions assumed in the IIASA scenarios. Nevertheless, climate change has to be taken into account when devising emission reduction policies for the future.

State-of-the-art models of the atmosphere are characterized by increasing complexity, but certainly still not all processes that have a distinct climate dependence are included. These include not only chemical reactions in air, but also microphysical processes, the pollutant uptake on vegetation and soil, various feedback mechanisms, etc. This has to be kept in mind when interpreting model responses to climate change.

Also, it has to be noted that the design of this experiment only allows investigation of effects from climate change on air pollution. For this purpose, CTMs, being computationally efficient, are useful tools as they can include, e.g. much more comprehensive chemistry modules than what is common in fully coupled chemistry-climate models. Nevertheless, calculations of the effect from air pollution on climate in addition do require a fully coupled model system. Therefore it is considered to use a fully coupled version of the Norwegian Earth System Model (NorESM) for climate-air pollution interaction studies at met.no and UiO in the future.

4) References

J. E Haugen and H.Haakenstad. The development of hirham version 2 with 50 km and 25 km resolution, 2006. RegClim General Technical Report No. 9, 159-173.

J. E. Haugen and T. Iversen. Response in extremes of daily precipitation and wind from a downscaled multi-model ensemble of anthropogenic global climate change scenarios. Tellus A, 60(3):411–426, 2008.

N.Nakicenovic and R. Swart, editors. Special Report on Emissions Scenarios. A Special Report of Working Group III of the Intergovernmental Panel on Climate Change. Cambridge University Press, Cambridge, United Kingdom and New York, NY, USA, 2000.

S. Solberg, O.Hov, A. Sovde, I. S.A. Isaksen, P.Coddeville, H.DeBacker, C. Forster, Y.Orsolini, and K.Uhse. European surface ozone in the extreme summer 2003. J. Geophys. Res., 113(D7), APR 10 2008. ISSN 0148-0227. doi: 10.1029/2007JD009098.

P. van der Linden and J. F. B.Mitchell, editors. ENSEMBLES: Climate change and its impacts: Summary of research and results from the ENSEMBLES project. Met Office Hadley Centre, Fitz-Roy Road, Exeter EX1 3PB, UK, 2009.